Highlight Review

Self-assembly and Nanostructure Formation of Multi-functional Organic π-Donors

Masahiko Iyoda,* Masashi Hasegawa,† and Hideo Enozawa

(Received October 17, 2007; CL-078009)

Abstract

Self-assembly of tetrathiafulvalenes, their conjugated oligomers, and giant macrocyclic oligothiophenes in solution leads to important solvatochromic, thermochromic, electrochromic, and switching properties. Furthermore, based on the self-assembly in solution, various nanostructures can be constructed in the solid state to produce nanowires, nanoparticles, nanotubes, tapes, ribbons, and microcrystals. This article highlights the self-aggregation of organic π-donors in solution and the formation of nanostructures from these π-donors in the solid state.

Introduction

Self-assembly of organic π-conjugated systems into complex, organized supramolecular structures via specific intermolecular interactions is a promising way to realize functional molecular materials.[1–3] Many intermolecular interactions such as hydrogen bonding,[4] metal coordination,[5] CT interaction,[6] and π–π stacking[7] have been utilized recently to construct desired supramolecular architectures such as fibers, ribbons, tapes, nanotubes, and nanoparticles.[1,8–10] Recently, we have developed a new concept of self-assembly by the use of cooperative S···S and π–π stacking interactions.[11] Although S···S interaction is a weak attractive force in solution, it plays an important role in packing of molecules in crystals.[12] Thus, organic conductors and superconductors based on tetrathiafulvalenes (TTF) are constructed using cooperative S···S and π–π stacking interactions.[13]

Crystal engineering of organic conductors suggests that van der Waals and dipole–dipole interactions between neutral sulfur atoms give rise to an attractive force in crystals.[14] The corresponding interactions in the oxidation state are also energetically favorable. Therefore, two TTF molecules tend to align face-to-face to produce a stacking structure in crystals.[15] Although the closely located dimeric TTF/TTF is weakly stable in the neutral state, the dimeric $\mathrm{TTF/TTF^{\cdot +}}$ is strongly stabilized in the cationic state to produce a mixed-valence form and hence the appearance of conductivity in the solid state.[16] Moreover, two cation–radicals $\mathrm{TTF^{\cdot +}/TTF^{\cdot +}}$ also interact attractively (π-dimer formation) in solution leading to the formation of a Mott-insulating semi-conductor in the solid state.[17] TTF can be converted into its dication $\mathrm{TTF^{2+}}$; however, two dications interact repulsively and form no stacking dimer.[18]

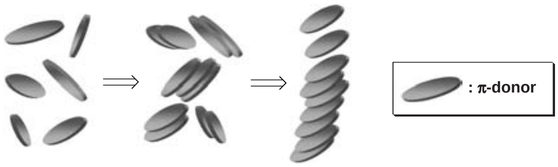

Figure 1. Self-aggregation and nanostructure formation of π-donors.

Although the conductive properties of TTF and its end-capped derivatives have extensively been investigated to realize highly conductive and superconducting radical salts,[19] self-assembly and nanostructures constructed by TTFs have not yet been completely elucidated except for the formation of bis-arborol–TTF gel[20] and the so-called "fastener effect" of TTF derivatives with long alkyl chains.[21] Recently, the production of electroactive nanowires from gelators having TTF moieties have been reported,[22,23] although such nanowires exhibit moderate to poor conductivities presumably due to their poor ability to form a good conduction path in the oxidized state.

It is known that π-conjugated molecules with either electron-withdrawing or large π-circles and disks self-aggregate in solution,[24] while the surface organization of π-conjugated molecules is frequently used by material scientists employing organic materials as molecular switches and devices.[25,26] To design a π-donor molecules with these applications, detailed knowledge of the structures of self-aggregates in solution or in mesophase is required, because pre-aggregation of conjugated π-systems may control the arrangement of the molecules on the solid surface. With this in mind, construction of a redox-active nanoscale architecture in solution and in the solid state has been achieved, and structures of neutral and cationic aggregates based on TTF oligomers and macrocyclic oligothiophenes have been investigated as a sulfur-rich π-system (Figure 1).

In this review, aggregation and self-assembly, control of one-, two-, and three-dimensional arrangements, and nanostructure formation of photochemically and electrochemically active TTFs and cyclic oligothiophenes will be focused on.

Gelation and Fiber Formation of Simple TTF derivatives

TTF derivatives with a long alkyl chain self-aggregate into a

---

Prof. Masahiko Iyoda, Dr. Masashi Hasegawa, Dr. Hideo Enozawa,*
Department of Chemistry, Graduate School of Science and Engineering, Tokyo Metropolitan University,
Hachioji, Tokyo 192-0397
E-mail: iyoda@tmu.ac.jp
†Present address: Department of Chemistry, School of Science, Kitasato University,
Sagamihara, Kanagawa 228-8555

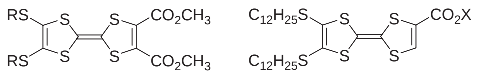

1a: R = $C_{12}H_{25}{}^n$
1b: R = $C_{18}H_{37}{}^n$
1c: R = CH_3

2a: X = CH_3
2b: X = H
2c: X = $N^+Bu_4{}^n$

Chart 1.

one-dimensional columnar structure in the solid state and show semi-conductive properties (fastener effect).[21,27] To utilize this effect in the construction of electroactive nanostructures, we focused on known simple amphiphilic TTF derivatives **1a**, **1b**, and **2a**–**2c** (Chart 1). Although these molecules have already been employed by several groups as synthetic precursors of functional π-systems, no significant properties of **1a**, **1b**, and **2a**–**2c** have been reported except for their enhanced solubility.[28,29] Since **1a**, **1b**, **2a**, and **2b** easily form a gel from nonpolar hydrocarbon solvents,[30] we expected a self-assembling fiber formation by intuition and reexamined nanostructures constructed by these amphiphilic TTF derivatives with extremely simple structures.[31]

The ^{1}H NMR and UV–vis spectra of TTF–esters **1a**–**1c** and **2a** showed no concentration dependence, suggesting no self-aggregation of these compounds in $CDCl_3$ and CD_2Cl_2. Similarly, a dilute solution of TTF–carboxylic acid **2b** in $CDCl_3$ or CD_2Cl_2 showed no concentration dependence. In contrast, as expected, **2b** revealed a monomer–dimer equilibrium in cyclohexane based on vapor pressure osmometric analysis.

As mentioned above, diesters **1a** and **1b** exhibited a gelling ability for hexane with a formation of a fibrous superstructure (Figures 2a and 2b). Thus, a warm solution of **1b** in hexane gradually changed to form a gel at room temperature (Figure 2a). The **1b** fibers were estimated to be about 2–5 µm in diameter and 1–10 mm in length by SEM and AFM measurements, indicating micron-fiber formation. XRD profiles of **1a** and **1b** fibers exhibited a regular reflection pattern, reflecting a considerably high crystallinity and the existence of a lamellar structure of head-to-head or head-to-tail dimers. In contrast, **2a** showed no gelation for the common organic solvents, and a yellow fibrous material was formed from acetonitrile. A SEM image of **2a** fibers revealed a tape-like morphology with fibers having 2–10-µm width and 100–1000-nm thickness (Figure 2c), although the XRD profile of **2a** tapes is similar to those of **1a** and **1b** fibers.

Carboxylic acid **2b** also gelated hexane ($>10\,\mathrm{mg\,cm^{-1}}$) and cyclohexane ($>30\,\mathrm{mg\,cm^{-1}}$) at room temperature to produce a reddish-orange gel (Figure 3a), and the microscopic image of xerogel of **2b** showed the formation of nanofibers (Figure 3b). Although ionic amphiphilic systems often exhibit gel formation,[1] the ammonium carboxylate **2c** showed no gelation or fiber formation from the common organic solvents and produced microcrystals from cyclohexane (Figure 3c).

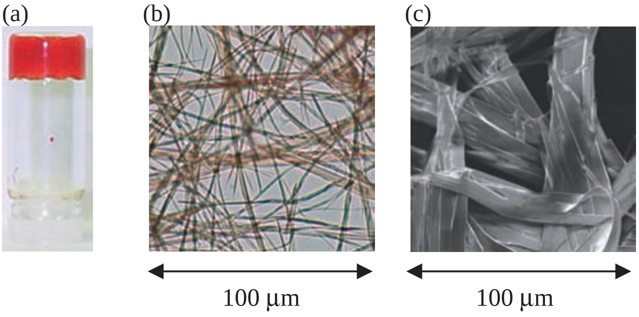

Figure 2. (a) **1b** gel from hexane ($10\,\mathrm{mg\,cm^{-3}}$). (b) Optical micrograph of **1b** xerogel. (c) SEM picture of tape-like structure of **2a** in CH_3CN ($2\,\mathrm{mg\,cm^{-3}}$).

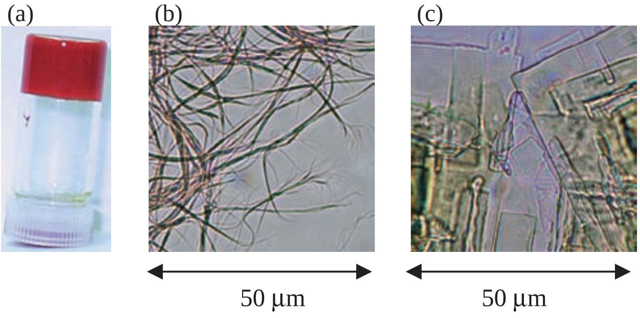

Figure 3. (a) **2b** gel from cyclohexane ($30\,\mathrm{mg\,cm^{-3}}$). (b) Optical micrograph of **2b** xerogel. (c) Optical micrograph of microplates of **2c** from cyclohexane ($10\,\mathrm{mg\,cm^{-3}}$).

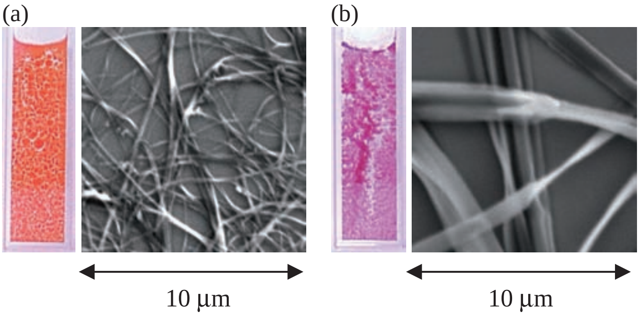

Figure 4. (a) Reddish-orange **2b** fibers from dilute hexane solution and SEM image thereof. (b) Reddish-violet **2b** fibers from dilute CH_3CN solution and SEM image thereof.

Note that the colors of **2b** fibers prepared from hexane and acetonitrile are quite different (Figure 4), although both XRD profiles are similar. Thus, **2b** shows solvatochromism both in solution and in the fiber formation. SEM and AFM images of **2b** fibers revealed that the reddish-orange fibers from hexane (50–500-nm width and 20–100-nm thickness) are smaller than those from acetonitrile (1–2-µm width and 100–1000-nm thickness). Since the alkyl–alkyl interaction in acetonitrile should be stronger than that in hexane and cyclohexane due to solvophobic effect, a stronger alkyl–alkyl overlap in an acetonitrile solution results in a shorter pitch of the lamellar structure, probably leading to a closer J-type stacking of the TTF moieties in **2b** and a marked color change of fibrous materials prepared from hexane and acetonitrile.

The TTF–diesters **1a** and **1b** showed reversible two-step redox potentials based on the TTF moiety. Although the first oxidation potentials of **1a** and **1b** are 0.33 V higher than that of TTF, the instability of the cation radicals $\mathbf{1a}^{\bullet+}$ and $\mathbf{1b}^{\bullet+}$ can be utilized as a molecular switch. Thus, a compressed **1b** pellet shows an electric conductivity of $\sigma_{\mathrm{rt}} = 2 \times 10^{-5}\,\mathrm{S\,cm^{-1}}$, doped with iodine vapor for 5 min, and the doped pellet becomes an insulator in air. This on–off procedure can be repeated several times without **1b** decomposition.

Published on the web (Advance View) November 17, 2007; doi:10.1246/cl.2007.1402

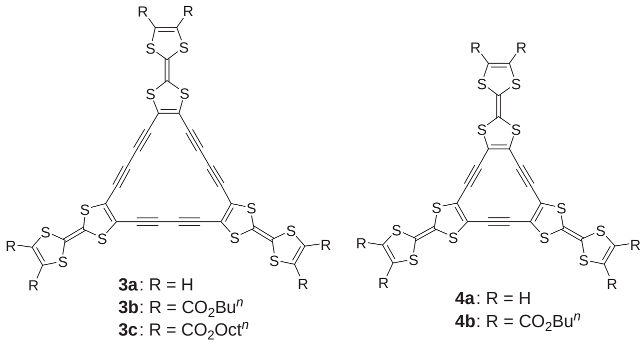
3a: R = H
3b: R = CO_2Bu^n
3c: R = CO_2Oct^n
4a: R = H
4b: R = CO_2Bu^n

Chart 2.

◆ Self-assembly and Chromic Properties of TTF–Annulenes

Recently, TTF-containing oligomers, polymers, and dendrimers have been synthesized to realize redox-active supramolecular structures.[15,32] In particular, conjugated TTF oligomers can be regarded as a candidate for a building block of supramolecular systems, because of their unique electronic properties in the neutral, radical-cationic, and poly-cationic states.[33] In 1998, Rubin and co-workers first proposed tris(tetrathiafulvaleno)dodecadehydro[18]annulene (**3a**) as a new class of π-donor molecule with enhanced dimensionality on MO calculations at PM3 level (Chart 2).[34] In parallel to that work, we reported the synthesis and properties of TTF-substituted dehydro[12]- and [20]annulenes.[35] In the course of our study on TTF–annulenes, the syntheses of the TTF–[18]annulenes **3b** and **3c** and TTF–[12]annulene **4b** were carried out using improved palladium-mediated coupling reactions.[36] These annulenes show unusual chromic properties based on their self-aggregation behavior in solution and form various morphologies in the solid state, depending on the conditions employed.

The aggregation of **3b**, **3c**, and **4b** in solution was systematically investigated by concentration/temperature-dependent ^{1}H NMR measurements in toluene-d_8, together with VPO analysis. Assuming a monomer–dimer equilibrium, the [18]annulene **3b** exhibits stronger aggregation than the [12]annulene **4b**, suggesting a higher stacking ability of **3b** based on its larger ring size. The aggregation ability of **3c** with longer alkyl chains is also strong compared with that of **3b**, due to the enhanced solvophobic effect (Table 1).

Although the electronic spectra of the annulenes **3b**, **3c**, and **4b** in benzene or toluene show almost no concentration dependence due to the low content of the aggregates in a dilute solution at room temperature, a film of **3b** or **3c** prepared from a benzene solution exhibits a red shift of the longest absorption maximum in the visible region with a color change from red (solution) to violet (film), suggesting the formation of π-stacked aggregates in the solid state. Since these aggregation behaviors are based on thermodynamic equilibrium, the ratio of the number of monomers to the number of dimers in solution can be controlled reversibly by changing temperature. Thus, the annulenes are expected to show "thermochromism." As shown in Figure 5, the color of a dilute solution of the [18]annulene **3c** in toluene changes from red at room temperature to violet at −78 °C. In this temperature range, a marked change of monomer/dimer ratio for **3c** is evidenced by thermodynamic parameters shown in Table 1.[37] A similar result was also obtained for **3b** with short alkyl chains, although the [12]annulene **4b** exhibited almost no color-changing behaviors due to the weakness of absorption in the visible region, reflecting the characteristics of a $4n\pi$ electronic structure.

Table 1. Association constants and thermodynamic parameters for dimerization of **3b**, **3c**, and **4b** in toluene-d_8[a]

Compounds	K_2 /M^{-1}[b]	ΔH /kJ·mol^{-1}	ΔS /J·mol^{-1}·K^{-1}
3b	317 ± 21	−37.8	−77.0
3c	321 ± 35	−48.0	−111
4b	110 ± 4.5	−32.0	−66.3

[a]Determined by ^{1}H NMR method. [b]At 303 K.

Interestingly, the [18]annulene **3b** formed a fibrous superstructure in aqueous THF media (Figure 6), while well-dispersed single molecules of **3b** were observed on a Au(111) surface, cast with a dilute solution of **3b** in CH_2Cl_2, by STM measurements. The fibers were estimated to be about 50–500 nm in width (SEM) and 20–100 nm in thickness (AFM). Furthermore, the assembled fibers were quite long and flexible, thus forming a complicated network. This fibrous material is readily soluble in THF, and the starting **3b** can be recovered without decomposition. Taking into account the molecular size, it was determined that 500–1000 strands of stacked molecular wire of **3b** form the nano-size fibrous structure.

Since the annulenes **3b**, **3c**, and **4b** are multi-redox systems with a donor (TTF)–acceptor (dehydroannulene) combination, conductive properties can also be expected in the solid state. Thus, doping of iodine into a pellet of **3b** fibers produced black cation radical salt which showed a fairly high electric conductivity of 2×10^{-2} S cm^{-1}.

◆ Self-assembly and Fiber Formation of Star-shaped TTF-oligomers

Star-shaped molecules such as tri-, tetra-, and hexa(ethynyl)benzene derivatives exhibit unique molecular structures and functional properties.[38] Moreover, self-assembly of star-shaped molecules can produce attractive supramolecular architectures.[39] To achieve anchoring of the star-shaped molecules in solution and in the solid state, our approach is to introduce

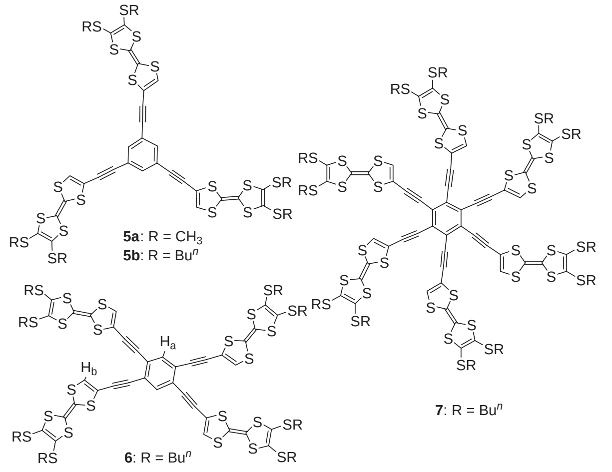
5a: R = CH_3
5b: R = Bu^n
6: R = Bu^n
7: R = Bu^n

Chart 3.

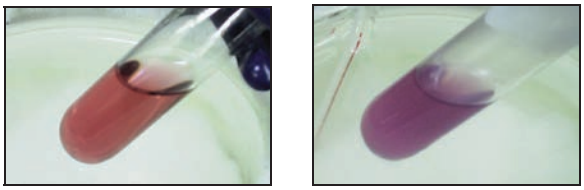

Figure 5. Colors of solution of **3c** in toluene (2.5×10^{-5} M) at room temperature (left) and −78 °C (right).

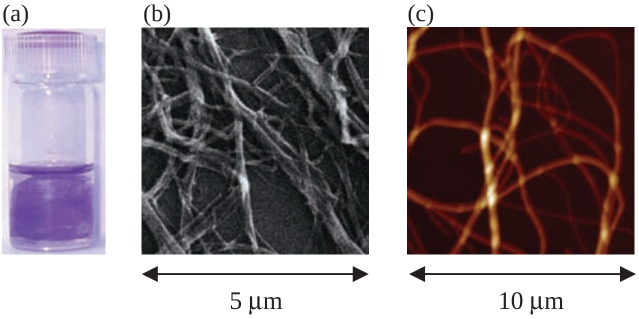

Figure 6. (a) Dispersed **3b** fibers in THF–H_2O (1:1). (b) SEM picture of **3b** fibers. (c) AFM image of **3b** fibers.

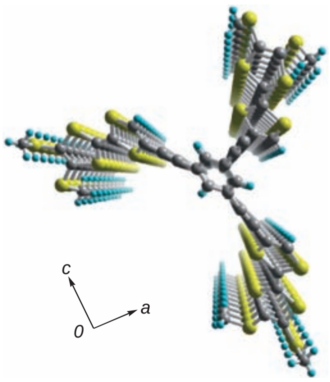

Figure 7. Packing structure of **5a** along the *b* axis.

TTF units as terminal substituents of poly(ethynyl)benzenes.[40,41] As shown in Chart 3, we synthesized a series of star-shaped TTF oligomers **5**–**7** and investigated the self-assembly and formation of nanostructures.[15a,40,41]

Although neutral TTF trimers **5a** and **5b** weakly aggregate in a $CDCl_3$ solution at room temperature, the stronger stacking of the cationic counterparts takes places under the same conditions using cooperative interactions of the three $TTF^{\bullet+}$ units (mixed-valence and π-dimer interactions).[40] In the solid state, the X-ray analysis of neutral **5a** shows a columnar structure (Figure 7), reflecting the three-fold face-to-face stacking interaction of the TTF units.

The neutral TTF tetramer **6** shows stronger stacking than **5b** in solution owing to the four-fold face-to-face interaction of the TTF units.[15a] As shown in Figure 8, the ^{1}H NMR spectra of **6** in $CDCl_3$ show both concentration- and temperature-dependences. The upper-field shift of the aromatic proton of **6** in concentrated solutions or at lower temperatures clearly indicates the face-to-face geometry of the central aromatic rings. Thus, although S···S and π–π stacking interactions between two neutral TTF molecules are weak in solution, **6** shows a fairly strong aggregation in solution at room temperature.

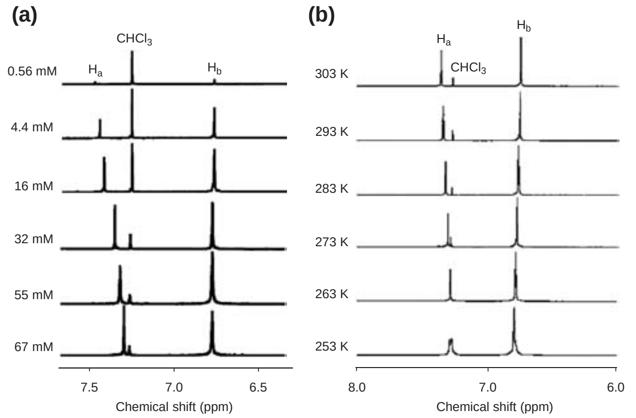

Figure 8. Concentration- and temperature-dependence of the ^{1}H NMR spectra of **6** in $CDCl_3$. (a) Measured in $CDCl_3$ at 25 °C. (b) Concentration: 50 mM in $CDCl_3$.

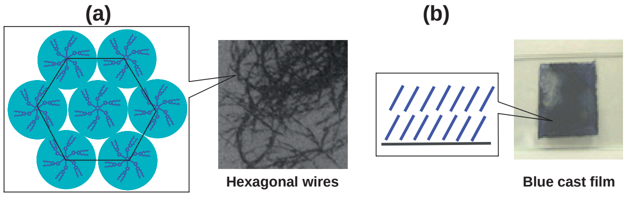

Figure 9. (a) Hexagonal **7** wires from $CHCl_3$–hexane. (b) Cast film of **7** on a glass surface.

By considering the self-aggregation of neutral **5** and **6**, hexakis(tetrathiafulvalenylethynyl)benzene (**7**) was designed as an ideal molecule to construct larger aggregates and nanostructures.[41] Since the six TTF units of **7** cooperatively work for S···S and π–π stacking interactions, **7** can show strong self-aggregation behavior. The unique TTF hexamer **7** was synthesized by modified Sonogashira reaction in good total yields. The TTF hexamer **7** strongly self-aggregates in $CHCl_3$ ($K_a = 2.1 \times 10^4$ M^{-1}, 23 °C), although **7** has a flexible disk-like molecular structure. Interestingly, **7** forms hexagonally ordered nanowires from a $CHCl_3$–hexane solution, while a cast film of **7** shows a different morphology such as lamellar structure vertical to the substrate and exhibits weak FET properties (Figure 9).

Selective oxidation of **7** with $Fe(ClO_4)_3$ forms the analytically pure monocation $\mathbf{7}^{\bullet+}ClO_4^-$ and trication $\mathbf{7}^{3+}(ClO_4^-)_3$. These cationic species strongly self-aggregate in $CHCl_3$ ($K_a = 2.3$–2.5×10^6 M^{-1}) and weakly aggregate in THF. However, the stacked cylindrical structures of these cationic species with a radius of 11 Å and a height of 14–16 Å were observed in THF. Furthermore, although fabrication of nanowires based on organic ion radicals has been scarcely reported, we succeeded in constructing hexagonally ordered nanowires of the monocation $\mathbf{7}^{\bullet+}ClO_4^-$ from $CHCl_3$–hexane solution, probably owing to the strong aggregation properties and molecular shape of $\mathbf{7}^{\bullet+}ClO_4^-$. In contrast, a cast film of $\mathbf{7}^{\bullet+}ClO_4^-$ shows a lamellar structure vertical to the substrate. Interestingly, the difference between nanowires and a film of $\mathbf{7}^{\bullet+}ClO_4^-$ leads to the different electric conductivities of wires (1.1×10^{-3} S cm^{-1}) and film (3.1×10^{-5} S cm^{-1}).

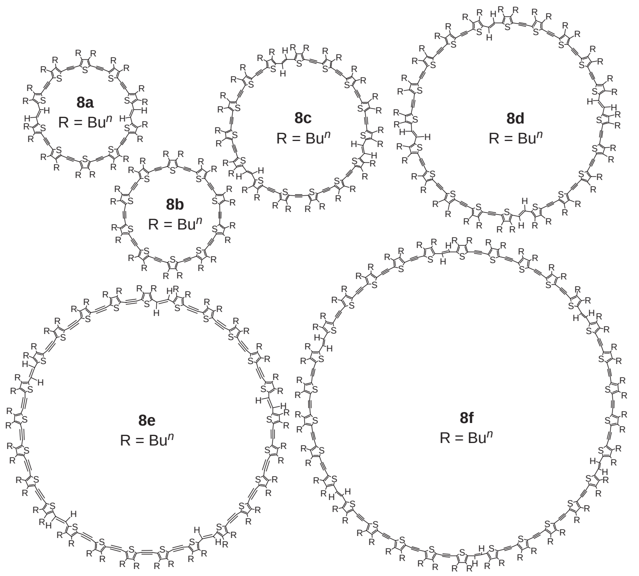

Chart 4.

◆ *Giant Macrocyclic Oligothiophenes*

Size- and shape-persistent macrocyclic oligoarylenes, heteroarylenes, and their π-expanded derivatives are regarded as an infinite π-conjugated system with an inner cavity,[42,43] and hence giant cycles attract considerable attention from the viewpoint of single-molecule electronics and unusual electronic properties.[44] Although fully conjugated macrocyclic molecules having a molecular size within 30 Å have been reported by several groups, a limited number of π-expanded macrocyclic oligoheteroarylenes and oligothiophenes with full conjugation have been investigated to date.[45,46] We designed and synthesized giant macrocyclic π-expanded oligothiophenes **8a**–**8f** (Chart 4).[47]

Fully conjugated giant macrocyclic oligothiophenes with 60π-, 90π-, 120π-, 150π-, and 180π-frames (**8a**–**8f**) have been synthesized using modified Sonogashira and McMurry coupling reactions as key steps. The 60–180π systems **8a**–**8f** are circular with 1.8–6.0 nm inner cavities and 3.3–7.5 nm outside molecular diameters. Compound **8a** containing ten 3,4-dibutyl-2,5-thienylene, eight ethynylene, and two vinylene units has been converted into macrocyclic oligo(3,4-dibutyl-2,5-thienylene-ethynylene) **8b** using a bromination–dehydrobromination procedure.

Giant macrocycles **8a**–**8f** exhibit a red shift of their absorption spectra (λ_{max}: 442–488 nm) and a fairly strong fluorescence (λ_{em}: 537–605 nm) with a large Stokes shift as compared with a linear conjugated reference compound having five thiophene rings. Compounds **8a**–**8f** exhibit multistep reversible redox behaviors with fairly low first oxidation potentials at 0.29–0.43 V vs. Fc/Fc$^+$, reflecting their cyclic conjugation. Furthermore, chemical oxidation of **8a**–**8f** with $\mathrm{FeCl_3}$ shows marked changes in spectroscopic properties due to intramolecular and intermolecular π–π interactions of giant macrocycles.

X-ray analysis of **8a** confirmed a round, planar structure with a nanoscale inner cavity, and revealed host ability for heptane and a unique packing structure (Figure 10).[48] Interestingly, **8c** and **8d** self-aggregate in the solid state to form fibrous materials (Figures 11a and 11b), which are about 200-nm thick and more than 1-mm long. The internal structures of fibrous aggregates have been investigated by optical microscope, SEM, AFM, and XRD analyses.[49] In contrast to crystal and fiber formations of **8a**, **8c**, and **8d**, larger macrocycles **8e** and **8f** form nanoparticles with a size of 300–800 nm (Figures 11c and 11d).

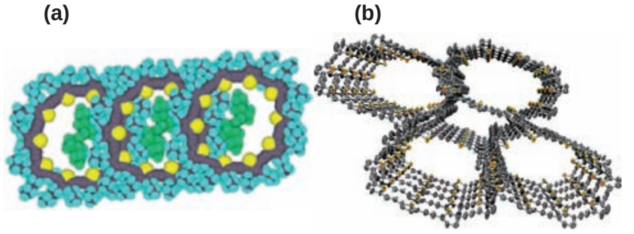

Figure 10. Crystal structure of **8a**. (a) Top view of three **8a**•heptane units. (b) Columnar packing structure (butyl groups and included heptanes are omitted for clarity).

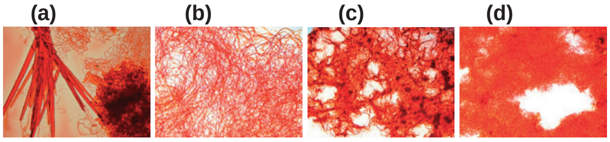

Figure 11. Microscopic images of **8c** (a), **8d** (b), **8e** (c), and **8f** (d) with 1000× magnification.

As mentioned above, all giant macrocycles show relatively low oxidation potentials, and hence doping of **8a**, **8c**, and **8d** with iodine forms semiconductors (**8a**: $1.86 \times 10^{-3}\ \mathrm{S\,cm^{-1}}$; **8c**: $2.63 \times 10^{-3}\ \mathrm{S\,cm^{-1}}$; **8d**: $2.03 \times 10^{-3}\ \mathrm{S\,cm^{-1}}$), indicating their π–π stacking structure.

◆ *Summary and Future Outlook*

Definite information about self-assembly of conjugated organic π-donors in solution is indispensable for precise control of molecular ordering in the solid state and solid–liquid interface. A variety of electroactive nanostructures can be fabricated on the basis of the self-assembly of these π-donors. The present article outlined the self-assembly and nanostructure formation of TTFs, their oligomers, and giant macrocyclic oligothiophenes. Simple amphiphilic TTF–esters **1a** and **1b** revealed gelation and nano- to micronfiber formation, whereas TTF–carboxylic acid **2b** showed solvatochromism in the fiber formation. TTF–annulenes **3b** and **3c** showed thermochromism and fiber formation. Interestingly, thermochromism of the annulenes reflects the monomer–dimer equilibrium. Star-shaped TTF–oligomers **5** and **6** exhibited concentration-dependence and temperature-dependence of ^{1}H NMR spectra, and **7** revealed strong stacking properties to form nanowires in the solid state. Furthermore, a film of **7** showed a lamellar structure vertical to the substrate and exhibited weak FET properties. In contrast to common organic cation radicals, $\mathbf{7}^{\cdot+}\mathrm{ClO_4}^-$ formed hexagonal nanofibers which revealed fairly high electric conductivity. Giant macrocyclic oligothiophenes showed unique structures and different morphologies depending on their ring size. Since conductive nanowires and nanoparticles may be employed for the fabrication of nanoswitches and nano-devices in the near future, the availability of these nanowires and nanoparticles should promote the development of effective nano-switches and nano-devices.

We gratefully acknowledge the Ministry of Education, Culture, Sports, Science and Technology, Japan for the financial support from Grant-in-Aid for Scientific Research.

This paper is dedicated to the memory of the Emeritus Professor Yoshihiko Ito of Kyoto University.

References and Notes

1 F. J. M. Hoeben, P. Jonkheijm, E. W. Meijer, A. P. H. J. Schenning, *Chem. Rev.* **2005**, *105*, 1491.

2 J. Wu, W. Pisula, K. Müllen, *Chem. Rev.* **2007**, *107*, 718.

3 D. M. Vriezema, M. C. Aragonés, J. A. A. W. Elemans, J. J. L. M. Cornelissen, A. E. Rowan, R. J. M. Nolte, *Chem. Rev.* **2005**, *105*, 1445.

4 a) M. L. Bushey, T.-Q. Nguyen, W. Zhang, D. Horoszewski, C. Nuckolls, *Angew. Chem., Int. Ed.* **2004**, *43*, 5446. b) L. Brammer, *Chem. Soc. Rev.* **2004**, *33*, 476. c) I. Huc, *Eur. J. Org. Chem.* **2004**, 17.

5 a) M. Ruben, J. Rojo, F. J. Romero-Salguero, L. H. Uppadine, J.-M. Lehn, *Angew. Chem., Int. Ed.* **2004**, *43*, 3644. b) S. Kitagawa, R. Kitaura, S. Noro, *Angew. Chem., Int. Ed.* **2004**, *43*, 2334. c) H. Hofmeier, U. S. Schubert, *Chem. Soc. Rev.* **2004**, *33*, 373. d) F. Würthner, C.-C. You, C. R. Saha-Möller, *Chem. Soc. Rev.* **2004**, *33*, 133. e) M. Oh, G. B. Carpenter, D. A. Sweigart, *Acc. Chem. Res.* **2004**, *37*, 1.

6 a) J. A. Marsden, J. J. Miller, L. D. Shirtcliff, M. M. Haley, *J. Am. Chem. Soc.* **2005**, *127*, 2464. b) A. R. Pease, J. O. Jeppesen, J. F. Stoddart, Y. Luo, C. P. Collier, J. R. Heath, *Acc. Chem. Res.* **2001**, *34*, 433.

7 M. D. Watson, A. Fechtenkotter, K. Müllen, *Chem. Rev.* **2001**, *101*, 1267.

8 T. Shimizu, M. Masuda, H. Minamikawa, *Chem. Rev.* **2005**, *105*, 1401.

9 a) Y. Yamamoto, T. Fukushima, A. Saeki, S. Seki, S. Tagawa, N. Ishii, T. Aida, *J. Am. Chem. Soc.* **2007**, *129*, 9276. b) G. Zhang, W. Jin, T. Fukushima, A. Kosaka, N. Ishii, T. Aida, *J. Am. Chem. Soc.* **2007**, *129*, 719. c) Y. Yamamoto, T. Fukushima, Y. Suna, N. Ishii, A. Saeki, S. Seki, S. Tagawa, M. Taniguchi, T. Kawai, T. Aida, *Science* **2006**, *314*, 1761.

10 A. Ajayaghosh, V. K. Praveen, *Acc. Chem. Res.* **2007**, *40*, 644.

11 a) M. Iyoda, M. Hasegawa, K. Hara, J. Takano, E. Ogura, Y. Kuwatani, *J. Phys. IV France* **2004**, *114*, 455. b) M. Hasegawa, Y. Kuwatani, M. Iyoda, *J. Phys. IV France* **2004**, *114*, 505.

12 a) D. B. Werz, R. Gleiter, F. Rominger, *J. Am. Chem. Soc.* **2002**, *124*, 10638. b) J. P. Glusker, *Top. Curr. Chem.* **1998**, *198*, 1.

13 a) M. Bendikov, F. Wudl, D. F. Perepichka, *Chem. Rev.* **2004**, *104*, 4891. b) T. Mori, *Chem. Rev.* **2004**, *104*, 4947.

14 G. R. Desiraju, V. Nalini, *J. Mater. Chem.* **1991**, *1*, 201.

15 a) M. Iyoda, M. Hasegawa, Y. Miyake, *Chem. Rev.* **2004**, *104*, 5085. b) M. Iyoda, in *TTF Chemistry*, ed. by J. Yamada, T. Sugimoto, Kodansha & Springer-Verlag, Tokyo, **2004**, p. 177.

16 J. B. Torrance, B. A. Scott, B. Welber, F. B. Kaufman, P. E. Seiden, *Phys. Rev. B* **1979**, *19*, 730.

17 a) V. Khodorkovsky, L. Shapiro, P. Krief, A. Shames, G. Mabon, A. Gorgues, M. Giffard, *Chem. Commun.* **2001**, 2736. b) M. Iyoda, K. Hara, Y. Kuwatani, S. Nagase, *Org. Lett.* **2000**, *2*, 2217.

18 M. Iyoda, M. Hasegawa, Y. Kuwatani, H. Nishikawa, K. Fukami, S. Nagase, G. Yamamoto, *Chem. Lett.* **2001**, 1146.

19 a) *Handbook of Organic Conductive Molecules and Polymers*, ed. by H. S. Nalwa, John Wiley & Sons, Chichester, **1997**. b) J. M. Williams, J. R. Ferraro, R. J. Thorn, K. D. Carlson, U. Geiser, H. H. Wang, A. M. Kini, M. H. Whangbo, *Organic Superconductor*, Prentice Hall, Englewood Cliffs, NJ, **1992**.

20 M. Jørgensen, K. Bechgaard, T. Bjørnholm, P. Sommer-Larsen, L. G. Hansen, K. Schaumburg, *J. Org. Chem.* **1994**, *59*, 5877.

21 H. Inokuchi, G. Saito, P. Wu, K. Seki, T. B. Tang, T. Mori, K. Imaeda, T. Enoki, Y. Higuchi, K. Inaka, N. Yasuoka, *Chem. Lett.* **1986**, 1263.

22 T. L. Gall, C. Pearson, M. R. Bryce, M. C. Petty, H. Dahlgaad, J. Becher, *Eur. J. Org. Chem.* **2003**, 3562.

23 a) J. Sly, P. Kasák, E. Gomar-Nadal, C. Rovira, L. Górriz, P. Thorarson, D. B. Amabilino, A. E. Rowan, R. J. M. Nolte, *Chem. Commun.* **2005**, 1255. b) T. Akutagawa, K. Kakiuchi, T. Hasegawa, S. Noro, T. Nakamura, H. Hasegawa, S. Mashiko, J. Becher, *Angew. Chem., Int. Ed.* **2005**, *44*, 7283. c) T. Kitamura, S. Nakaso, N. Mizoshita, Y. Tochigi, T. Shimomura, M. Moriyama, K. Ito, T. Kato, *J. Am. Chem. Soc.* **2005**, *127*, 14769. d) T. Kitahara, M. Shirakawa, S. Kawano, U. Beginn, N. Fujita, S. Shinkai, *J. Am. Chem. Soc.* **2005**, *127*, 14980. e) C. Wang, D. Zhang, D. Zhu, *J. Am. Chem. Soc.* **2005**, *127*, 16372.

24 a) S. Höger, *Chem.—Eur. J.* **2004**, *10*, 1320. b) D. Zhao, J. S. Moore, *Chem. Commun.* **2003**, 807. c) Y. Yamaguchi, Z. Yoshida, *Chem.—Eur. J.* **2003**, *9*, 5430.

25 a) *Molecular Switches*, ed. by B. L. Feringa, Wiley-VCH Weinheim, **2001**. b) *Molecular Devices and Machines*, ed. by V. Balzani, M. Venturi, A. Credi, Wiley-VCH Weinheim, **2003**. c) A. C. Benniston, *Chem. Soc. Rev.* **2004**, *33*, 573. d) D. Wouters, U. S. Schubert, *Angew. Chem., Int. Ed.* **2004**, *43*, 2480.

26 V. Palermo, P. Samori, *Angew. Chem., Int. Ed.* **2007**, *46*, 4428.

27 Quite recently, a doped TTF–diamide was found to exhibit metallic-like spectroscopy curves when probed with current-sensing AFM: J. Puigmartí-Luis, A. Minoia, Á. P. del Pino, G. Ujaque, C. Rovira, A. Lledós, R. Lazzaroni, D. B. Amabilino, *Chem.—Eur. J.* **2006**, *12*, 9161.

28 a) M. González, N. Martín, J. L. Segura, J. Garín, J. Orduna, *Tetrahedron Lett.* **1998**, *39*, 3269. b) J. L. Segura, E. M. Priego, N. Martín, L. Luo, D. M. Guldi, *Org. Lett.* **2000**, *2*, 4021. c) I. Olejniczak, A. Graja, A. Bogucki, M. Golub, P. Hudhomme, A. Gorgues, D. Kreher, M. Cariou, *Synth. Met.* **2002**, *126*, 263.

29 M. M. S. Abdel-Mottaleb, E. Gomar-Nadal, M. Surin, H. Uji-i, W. Mamdouh, J. Veciana, V. Lemaur, C. Rovira, J. Cornil, R. Lazzaroni, D. B. Amabilino, S. De Feyter, F. C. De Schryver, *J. Mater. Chem.* **2005**, *15*, 4601.

30 For low-molecular-mass organic gelators (LMOGs), see: M. George, R. G. Weiss, *Acc. Chem. Res.* **2006**, *39*, 489.

31 a) Y. Kobayashi, M. Hasegawa, H. Enozawa, M. Iyoda, *Chem. Lett.* **2007**, *36*, 720. b) H. Enozawa, Y. Honna, M. Iyoda, *Chem. Lett.* **2007**, *36*, 1434.

32 a) J. L. Segura, N. Martín, *Angew. Chem., Int. Ed.* **2001**, *40*, 1372. b) M. R. Bryce, *J. Mater. Chem.* **2000**, *10*, 589. c) M. B. Nielsen, C. Lomholt, J. Becher, *Chem. Soc. Rev.* **2000**, *29*, 153.

33 a) M. Iyoda, S. Sasaki, M. Miura, M. Fukuda, J. Yamauchi, *Tetrahedron Lett.* **1999**, *40*, 2807. b) A. González, J. L. Segura, N. Martín, *Tetrahedron Lett.* **2000**, *41*, 3083.

34 D. Solooki, T. C. Parker, S. I. Khan, Y. Rubin, *Tetrahedron Lett.* **1998**, *39*, 1327.

35 a) K. Hara, H. Hasegawa, Y. Kuwatani, H. Enozawa, M. Iyoda, *Chem. Commun.* **2004**, 2042. b) M. Iyoda, H. Enozawa, Y. Miyake, *Chem. Lett.* **2004**, *33*, 1098.

36 H. Enozawa, M. Hasegawa, D. Takamatsu, K. Fukui, M. Iyoda, *Org. Lett.* **2006**, *8*, 1917.

37 At room temperature, **3c** exists mainly as monomeric form and the solution is red, whereas **3c** exists mainly as dimeric form at −78 °C and the solution is violet.

38 a) S. A. Ponomarenko, S. Kirchmeyer, B.-H. Huisman, A. Karbach, D. Drechsler, *Adv. Funct. Mater.* **2003**, *13*, 591. b) I. M. Saez, J. W. Goodby, *Chem.—Eur. J.* **2003**, *9*, 4869. c) M. Sonntag, K. Kreger, D. Hanft, P. Strohriegl, S. Setayesh, D. De Leeuw, *Chem. Mater.* **2005**, *17*, 3031. d) S. Roquet, A. Cravino, P. Leriche, O. Alévêque, P. Frére, J. Roncali, *J. Am. Chem. Soc.* **2006**, *128*, 3459. e) F. Ponzini, R. Zagha, K. Hardcastle, J. S. Siegel, *Angew. Chem., Int. Ed.* **2000**, *39*, 2323.

39 a) K. Heuzé, D. Méry, D. Gauss, J.-C. Blais, D. Astruc, *Chem.—Eur. J.* **2004**, *10*, 3936. b) H.-J. Kim, S. Sakamoto, K. Yamaguchi, J.-I. Hong, *Org. Lett.* **2003**, *5*, 1051. c) M. L. Bushey, A. Hwang, P. W. Stephens, C. Nuckolls, *J. Am. Chem. Soc.* **2001**, *123*, 8157.

40 a) M. Hasegawa, J. Takano, H. Enozawa, Y. Kuwatani, M. Iyoda, *Tetrahedron Lett.* **2004**, *45*, 4109. b) M. Iyoda, M. Hasegawa, J. Takano, K. Hara, Y. Kuwatani, *Chem. Lett.* **2002**, 590.

41 M. Hasegawa, H. Enozawa, Y. Kawabata, M. Iyoda, *J. Am. Chem. Soc.* **2007**, *129*, 3072.

42 a) S. Höger, *J. Polym. Sci., Part A: Polym. Chem.* **1999**, *37*, 2685. b) C. Grave, A. D. Schlüter, *Eur. J. Org. Chem.* **2002**, 3075. c) S. Höger, *Angew. Chem., Int. Ed.* **2005**, *44*, 3806. d) S. A. Dieter, *Top. Curr. Chem.* **2005**, *245*, 151. e) *Acetylene Chemistry*, ed. by F. Diederich, P. J. Stang, R. R. Tykwinski, Wiley-VCH Weinheim, **2005**.

43 a) M. Iyoda, M. J. Rahman, A. Matsumoto, M. Wu, Y. Kuwatani, K. Nakao, Y. Miyake, *Chem. Lett.* **2005**, *34*, 1474. b) Y. Miyake, M. Wu, M. J. Rahman, M. Iyoda, *Chem. Commun.* **2005**, 411.

44 a) A. Godt, S. Duda, Ö. Ünsal, J. Thiel, A. Härter, M. Roos, C. Tschierske, S. Diele, *Chem.—Eur. J.* **2002**, *8*, 5094. b) T. Hori, N. Aratani, A. Takagi, T. Matsumoto, T. Kawai, M.-C. Yoon, Z. S. Yoon, S. Cho, D. Kim, A. Osuka, *Chem.—Eur. J.* **2006**, *12*, 1319. c) F. Hajjaj, Z. S. Yoon, M.-C. Yoon, J. Park, A. Satake, D. Kim, Y. Kobuke, *J. Am. Chem. Soc.* **2006**, *128*, 4612.

45 M. Mayor, C. Didschies, *Angew. Chem., Int. Ed.* **2003**, *42*, 3176.

46 a) L. Krömer, I. Rios-Carreras, G. Fuhrmann, C. Musch, M. Wunderlin, T. Debaerdemaeker, E. Mena-Osteritz, P. Bäuerle, *Angew. Chem.* **2000**, *39*, 3481. b) E. Mena-Osteritz, P. Bäuerle, *Adv. Mater.* **2001**, *13*, 243.

47 a) K. Nakao, M. Nishimura, T. Tamachi, Y. Kuwatani, H. Miyasaka, T. Nishinaga, M. Iyoda, *J. Am. Chem. Soc.* **2006**, *128*, 16740. b) M. Iyoda, *Heteroat. Chem.* **2007**, *18*, 460.

48 Giant macrocycles **8a** and **8b** serve as a host molecule to alkane guests such as hexane, heptane, and octane.

49 Although XRD reflections of **8c**–**8f** exhibit similar patterns, their morphologies are different.